



# Liquid dosimeter with sensitivity in low-kGy range for the characterization of a new module for EB wastewater treatment

Lotte Ligaya Schaap ,  
Tobias Teichmann ,  
Andre Poremba,  
Joana Kira Besecke ,  
Simone Schopf ,  
Gösta Mattausch,  
Elizabeth von Hauff

**Abstract.** In recent years, the use of low-energy electrons in various ecological and biotechnological applications has become increasingly relevant. One important application is the treatment of wastewater, wherein highly reactive species produced by water irradiation are used to oxidize pollutants. Low-energy electron irradiation has several advantages, such as minimal demands on radiation protection and electron beam (EB) source dimensions. However, to play into the main advantages of this technology and keep it economically viable, it is necessary to keep the absorbed dose as low as possible. This calls for a liquid dosimeter with sensitivity in the single digit kGy range. An extract from natural *Hibiscus sabdariffa* (Roselle) has been reported to show a radiochromic effect in this dose range. In the present work, Roselle dosimeter solutions were closely investigated and optimized to characterize a new module for EB wastewater treatment. Upon EB irradiation, the dosimeter solution demonstrated a dose-dependent fading in color, making it useful in the 0.3–7.5 kGy dose range.

**Keywords:** Liquid dosimetry • Low-energy electrons • Radiochromic effects • Roselle

## Introduction

Electron beam (EB) is a versatile tool used in a wide range of applications. Among other examples, non-thermal electrons are used to achieve controlled chemical and biological effects in order to treat wastewater, inactivate pathogens, sterilize medical products, and irradiate blood components.

More recently, there has been a rising concern due to the presence of highly persistent micropollutants in hospital and municipal effluents. The presence of these substances in effluents pose numerous concerns, including ecological toxicity, antimicrobial resistance [1], endocrine disruption [2], and gradual reduction of fertility [3].

Currently, no treatment to eliminate the majority of emerging micropollutants simultaneously and reliably in the presence of traditional pollutants has been established. However, some advanced oxidation processes (AOPs), which utilize the OH radical, have demonstrated the ability to degrade some of these substances [2]. EB irradiation of wastewater falls into the category of AOPs, as this process produces several highly reactive, oxidizing, and reducing radical species [4], which can effectively degrade persistent pollutants or inactivate pathogens.

L. L. Schaap<sup>✉</sup>, T. Teichmann, A. Poremba,  
J. K. Besecke, S. Schopf, G. Mattausch, E. von Hauff  
Fraunhofer Institute for Electron Beam and Plasma  
Technology FEP, Dresden, Germany  
E-mail: lotte.ligaya.schaap@fep.fraunhofer.de

Received: 15 November 2023

Accepted: 3 April 2024

0029-5922 © 2024 The Author(s). Published by the Institute of Nuclear Chemistry and Technology.  
This is an open access article under the CC BY-NC-ND 4.0 licence (<http://creativecommons.org/licenses/by-nc-nd/4.0/>).

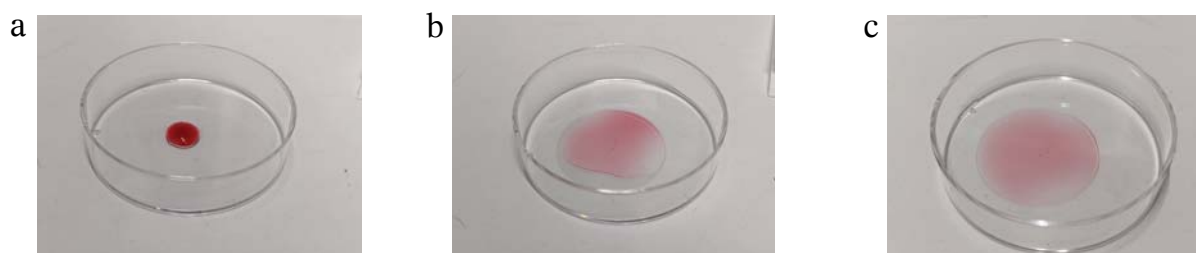


**Fig. 1.** Roselle dosimeter in oriented polypropylene setup.

Due to EB's ability to partially or completely inactivate pathogens at significantly lower energies, it has become an emerging alternative technology in many medical, biotechnological, and pharmaceutical applications [5]. The use of low-energy electrons has several advantages over traditional methods. For example, the inactivation of vaccines by EB has proved to be a much faster process, and predominantly damages nucleic acids while still conserving most of the antigenic structures [6].

Other applications include the irradiation of blood and blood components for suppression of T-lymphocytes, and for prevention of disorders such as graft-vs-host disease in immunodeficient patients [7]. The sterilization of medical devices and pharmaceuticals has also become an important commercial application for EB [4].

The chemical and biological effects induced by EB are mainly dependent on the absorbed dose [5]. Consequently, to keep this technology economically viable yet simultaneously effective, the absorbed dose must be minimized and precisely controlled. While liquid dosimetry systems such as Fricke, dichromate, and tetrazolium dosimeter exist, suitable liquid dosimeters which can measure the dose to treat wastewater in the medium dose range of 0.1–10 kGy are unavailable [8].

An investigation into the development of a simple dosimetry system using radiochromic liquid by Handayani and Imawan [9] revealed that the extract from *Hibiscus sabdariffa* (Roselle) has exhibited a radiochromic effect in this dose range. Roselle contains the natural dye anthocyanin, a renewable bioresource with minimal environmental and health impact [10]. Anthocyanins can be extracted in a simple procedure using a polar solvent.



## Methodology

### Sample preparation

The dosimeter solution was prepared according to Handayani and Imawan [9]. Preliminary experiments revealed that ethanol-solved Roselle had significant evaporation, interfering with measurements. The sample preparation was then adapted using deionized water instead of ethanol. The dosimeter solution was prepared using 20 g of Roselle extract soaked in 400 mL deionized water as a solvent. The solution was refrigerated at 8–10°C and sealed with aluminum foil for 24 h.

The solution was then filtered using filter paper (Whatman no. 1) and homogenized using a mechanical stirrer at 100 rpm for 30 min. The dosimeter solution was prepared fresh prior to irradiation.

### Irradiation of the samples

Irradiation was carried out in a four-Petri dish system by placing one 57  $\mu$ L drop of dosimeter solution in each Petri dish. A 50  $\mu$ m foil of oriented polypropylene (OPP) was then placed on top of each drop to generate a thin liquid layer (approximately 81  $\mu$ m), as shown in Fig. 1.

The samples were irradiated at FEP's laboratory facility REAMODE, equipped with an electron emitter with 200 keV maximum electron energy. The linear module, shown in Fig. 2, was used, allowing linear transport and height adjustment. The samples were passed eight times under the beam. For all irradiations, the acceleration voltage was set to 200 kV, the distance from the electron exit foil to

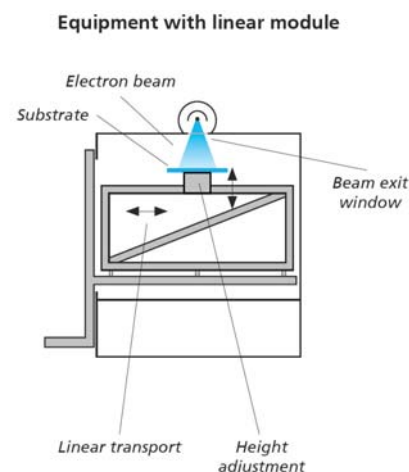


**Fig. 2.** FEP's laboratory EB facility REAMODE (left) with linear module (right).

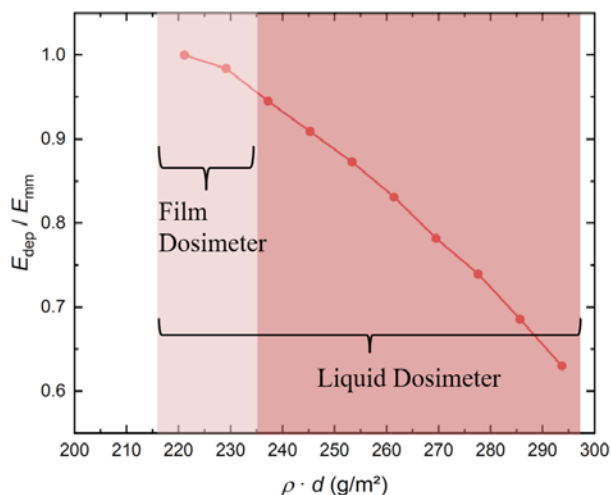


Fig. 3. Depth-dose distribution in the liquid layer.

the sample to 88 mm, and sample speed to 20 mm/s. Adjustments of irradiation doses were made by varying the beam current at 0–0.64 mA. Two batches of dosimeter solution were prepared, with three trials performed for Batch 1 and two trials performed for Batch 2.

Irradiated samples were pooled and absorption spectra of the dosimeter solution were measured by pipetting 100  $\mu$ L of the solution into wells of a 96-well plate (Greiner), with the readout done using Tecan infinite M200 from Tecan Group Ltd., at wavelengths from 400 nm to 800 nm.

The data were then processed and analyzed in order to obtain the absorbance spectrum of the dosimeter solution. Furthermore, the absorbance at peak and net absorbance were plotted as a function of the absorbed dose. Additionally, the short-time dependence and 4-day time dependence were investigated.

Dose measurements taken from calibrated radiochromic dosimeter film (Gafchromic HD-V2 high-dose dosimetry film, USA and Risø B3 dosimeter, Denmark) were used as a reference and represent the dose at the surface independent of the liquid layer. To account for the dose variations within the sample, the depth-dose distribution in the liquid layer

was reproduced using Monte Carlo simulations, as shown in Fig. 3. The average dose in the liquid layer was calculated using the surface dose and the depth-dose curve, resulting in a 16% decrease in the average dose in the liquid layer compared with the average dose in the film.

## Results and discussion

### Absorbance spectra of the dosimeter solution

Figure 4 shows the absorbance spectrum for each dose. The absorbance spectra of the dosimeter solution have a peak at 520 nm, in comparison to the spectra from Handayani and Imawan [9] which show a peak at 530 nm. This difference may be due to the use of different solvents during sample preparation, or the use of Roselle extract instead of dried Roselle flower. Nonetheless, the 520 nm peak indicates the presence of anthocyanins, as the prominent absorbance peak of anthocyanins usually lies at 500–550 nm [11, 12].

Identically, the spectra show a decrease in absorbance with an increase in dose. This occurs due to the anthocyanin molecule having hydroxide groups (OH), which release their hydrogen atoms as ions into water, upon irradiation [13]. Anthocyanins are usually represented by their flavylium cation, the predominant species at low pH, which gives the distinct red color of the solution [14]. Flavylium cations are easily deprotonated to form the colorless carbinol [15]. Correspondingly, the dosimeter solution presents a red color which fades upon EB irradiation, as shown in Fig. 5.

### Dosimetry system response and calibration

The dosimeter response is defined as the change in absorbance of the solution ( $\Delta A$ ) before irradiation ( $A_0$ ) and after irradiation ( $A_i$ ) at the maximum absorbance at 520 nm, and increases exponentially with respect to the dose [9]. The behavior can be modeled by the following function, where  $D$  is the dose (kGy), and  $a$  and  $b$  are model parameters:

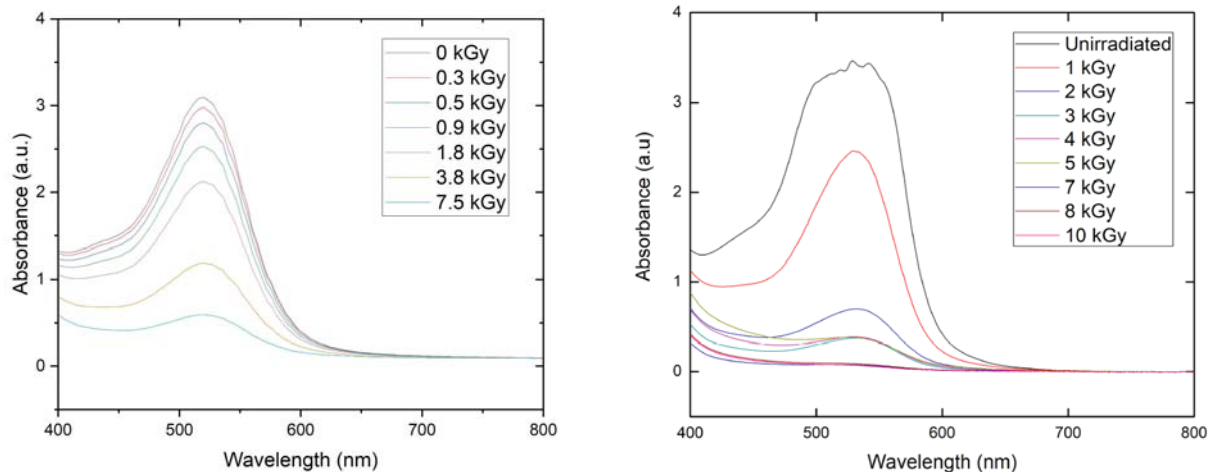


Fig. 4. Absorbance spectra of Roselle dosimeter at different doses (left) and absorbance spectra from Handayani and Imawan [9] (right).



**Fig. 5.** Roselle dosimeter irradiated at 0, 0.6, 1.3, and 2.5 kGy.

$$(1) \quad \text{Dosimeter response} = a * (1 - e^{-b*D})$$

Figure 6 shows the absorbance at the 520 nm peak plotted as a function of the absorbed dose, and the dosimeter response as a function of reference dose. As reported [9, 16], absorbance decreases exponentially with an increase in dose. The coefficient of determination (adjusted  $R^2$ ) for the exponential model was 0.99.

This dose-dependent exponential increase/decrease observed in Fig. 6 occurs due to the large concentration of anthocyanin molecules present before irradiation, which require larger doses to achieve significant degradation. As shown in the calibration curve, significant degradation occurs from 1.8 kGy to 3.8 kGy. This occurs at a higher dose compared with that of ethanol-solved Roselle, wherein the greatest dose response occurs at 0–3 kGy. It has been reported that the fading of color in water-solved Roselle is much slower compared with ethanol-solved Roselle,

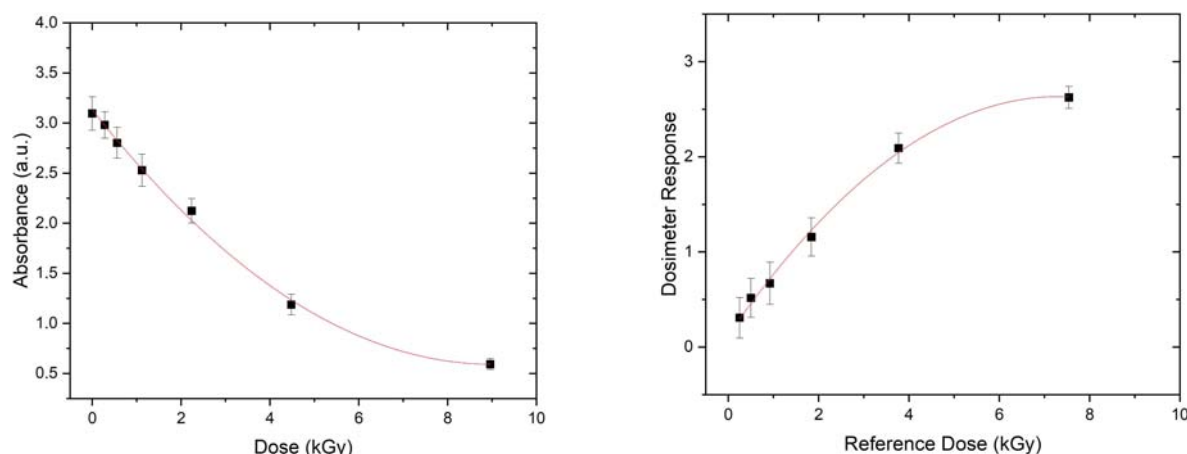


**Fig. 6.** Maximum absorbance of Roselle dosimeter at 520 nm peak vs. reference dose (left) and calibration curve of Roselle dosimeter: dosimeter response vs. reference dose (right).

**Table 1.** Relative change in peak absorbance of Roselle dosimeter solution at set time intervals. Negative values indicate a decrease in peak absorbance

Dose (kGy)	Peak absorbance	Relative change in peak absorbance (%)					
		10 min	20 min	30 min	40 min	1 h	96 h
0	3.74	0.6	3.9	4.1	-0.3	-1.1	-68.8
0.3	2.93	-0.5	-1.5	-2.2	-2.9	-8.3	-53.9
0.9	2.61	-1.3	-2.2	-3.1	-9.5	-9.5	-55.6
1.8	1.20	-0.7	-0.7	-1.5	-1.9	-12.1	-59.1
3.8	1.05	0.9	2.4	4.3	5.5	5.3	-3.2
7.5	0.51	5.0	10.6	15.9	21.0	42.1	21.4

due to anthocyanins being more stable in water [16]. As the dose is increased further, degradation decreases due to the decrease in concentration of anthocyanin, and at a certain point, a saturation dose will be reached, wherein all the molecules have been degraded and no color change occurs.

The variability observed between measurements is attributed to several factors such as the lack of control in anthocyanin pigments, evaporation, and deviations in the sample collection method.

#### Time dependence of the dosimeter response

The short-time dependence of the response was investigated by measuring the absorbance spectrum of the solution at certain time frames. This was done by irradiating a sample at the lowest dose of 0.3 kGy, then measuring the absorbance. Another sample was then irradiated at 0.9 kGy, its absorbance measured, while the absorbance of the 0.3 kGy sample was remeasured. This procedure was repeated as the dose was increased, with all the previous samples being remeasured as a new sample was added. The reverse was also done by starting from the highest dose of 7.5 kGy. Measurements were taken approximately 10 min apart. Absorbance measurements were also taken 1 h after irradiation. After investigation of the short-time dependence, the samples were sealed with aluminum foil and refrigerated at 8–10° for 4 days, and absorbance values were measured thereafter.

As shown in Table 1, the unirradiated solution remained stable over a 1 h time span, with a relative change in peak absorbance of <5%. The 7.5 kGy solu-

tion showed instability already at 10 min, increasing in absorbance by 5%. Minimal changes in peak absorbance of 0.5–4.3% occurred for solutions irradiated from 0.3 kGy to 3.8 kGy during the 10–30 min time interval. Although minimal, these uncertainties must be considered when evaluating dosimetric data, even when the readout is done directly after irradiation.

After 40 min, absorbance measurements for solutions irradiated at 0.3–3.8 kGy showed instability. After 4 days, the change in peak absorbance is over 50% for the majority of samples. The degradation and discoloration of the solution that occurs over time and during storage could be attributed to the anthocyanin molecule's stability, which is highly susceptible to external factors such as pH, temperature, oxygen, and light exposure [14].

The investigation on the time dependence suggests that absorbance measurements be taken immediately after irradiation. As the unirradiated sample remains stable over the short timescale, this would allow ample time for calibration before beginning dosimetry measurements.

### Conclusion and recommendation

The low-energy EB irradiation response of Roselle dosimeter solution was investigated. Decolorization of the solution and a dose-dependent change in absorbance spectra were observed. The Roselle dosimeter solution can be used as a liquid dosimeter in the range of 0.3–7.5 kGy. However, due to a short-time change of the irradiated dosimeter, it is recommended that the dosimeter solution is prepared fresh prior to irradiation, and that absorbance measurements are taken immediately after irradiation. When absorbance measurements were taken immediately, the relative standard deviation was measured as 9% ( $k = 1$ ). The sample irradiation and collection method must be optimized to further reduce this uncertainty.

**Acknowledgment.** This research is co-financed by the European Regional Development Fund and tax funds based on the budget passed by the Saxon state parliament and performed in a joint project with CREAVAC GmbH under grant no. 100534392 of the Development Bank of Saxony.

### ORCID

J. K. Besecke  <http://orcid.org/0009-0002-4280-7913>  
 E. von Hauff  <http://orcid.org/0000-0002-6269-0540>  
 L. L. Schaap  <http://orcid.org/0009-0001-4059-3889>  
 S. Schopf  <http://orcid.org/0000-0002-8462-7147>  
 T. Teichmann  <http://orcid.org/0000-0002-0331-3083>

### References

1. Szabó, L., Szabó, J., Illés, E., Kovács, A., Belák, A., Mohácsi-Farkas, C., Takács, E., & Wojnárovits, L. (2017). Electron-beam treatment for tackling the escalating problems of antibiotic resistance: Eliminating the antimicrobial activity of wastewater matrices originating from erythromycin. *Chem. Eng. J.*, 321, 314–324. DOI: 10.1016/j.cej.2017.03.114.
2. Capodaglio, A. (2019). Contaminants of emerging concern removal by high-energy oxidation-reduction processes: State of the art. *Appl. Sci.*, 9(21), 4562. DOI: 10.3390/app9214562.
3. Coleman, H. M., Abdullah, M. I., Eggins, B. R., & Palmer, F. L. (2005). Photocatalytic degradation of 17 $\beta$ -oestradiol, oestriol and 17 $\alpha$ -ethynyl-oestradiol in water monitored using fluorescence spectroscopy. *Appl. Catal. B-Environ.*, 55(1), 23–30. DOI: 10.1016/j.apcatb.2004.07.004.
4. Bluhm, H., Han, B., Chmielewski, A. G., von Döbeneck, D., Gohs, U., Gstöttner, J., Mattausch, G., Morgner, H., Koops, H. W. P., Reichmann, A., Röder, O., Schultz, S. W., Wenzel, B., & Zywitzki, O. (2008). Electron-beam devices for materials processing and analysis. In J. A. Eichmeier & M. Thumm (Eds.), *Vacuum electronics – components and devices* (pp. 155–224). Berlin, Heidelberg, New York: Springer Science & Business Media.
5. Schopf, S., Gotzmann, G., Dietze, M., Gerschke, S., Kenner, L., & König, U. (2022). Investigations into the suitability of bacterial suspensions as biological indicators for low-energy electron irradiation. *Front. Immunol.*, 13, 814767. DOI: 10.3389/fimmu.2022.814767.
6. Fertey, J., Bayer, L., Grunwald, T., Pohl, A., Beckmann, J., Gotzmann, G., Portillo Casado, J., Schönfelder, J., Rögner, F. -H., Wetzel, C., Thoma, M., Bailer, S. M., Hiller, E., Rupp, S., & Ulbert, S. (2016). Pathogens inactivated by low-energy-electron irradiation maintain antigenic properties and induce protective immune responses. *Viruses*, 8(11), 319. DOI: 10.3390/v8110319.
7. Jacobs, G. P. (1998). A review on the effects of ionizing radiation on blood and blood components. *Radiat. Phys. Chem.*, 53(5), 511–523. DOI: 10.1016/S0969-806X(98)00185-6.
8. McLaughlin, W. L., Miller, A., Kovács, A., & Mehta, K. K. (2011). Dosimetry methods. In A. Vértes, S. Nagy, Z. Klencsár, R. G. Lovas & F. Rösch (Eds.), *Handbook of nuclear chemistry* (2nd ed.) (Vol. 5, pp. 2287–2318). Boston: Springer Science & Business Media.
9. Handayani, I. N., & Imawan, C. (2018). Liquid radiochromic from Roselle dye extract for gamma-ray dosimetry applications at medium dose levels. In The 3rd International Seminar on Sensors, Instrumentation, Measurement and Metrology, 4–5 December 2018 (pp. 64–67). Depok, Indonesia: IEEE.
10. Shahid, M., Islam, S. ul, & Mohammad, F. (2013). Recent advancements in natural dye applications: a review. *J. Clean Prod.*, 53, 310–331. DOI: 10.1016/j.jclepro.2013.03.031.
11. Ramamoorthy, R., Radha, N., Maheswari, G., Anandan, S., Manoharan, S., & Williams, R. V. (2016). Betalain and anthocyanin dye-sensitized solar cells. *J. Appl. Electrochem.*, 46(9), 929–941. DOI: 10.1007/s10800-016-0974-9.
12. Suhaimi, S., Nasri, N. M., Wahab, S., Ismail, N. S., Shahimin, M. M., & Sauli, Z. (2020). Ultraviolet-

- visible absorbance analysis on solvent dependent effect of tropical plant anthocyanin extraction for dye-sensitized solar cells. *AIP Conf. Proc.*, 2203(1), 020054. DOI: 10.1063/1.5142146.
13. Akram, N. G., Bhutto, W. A., & Sharif, I. N. (2016). A study on the response of natural dye to gamma radiation as a dosimeter. *Afr. J. Chem.*, 3(3), 182–187.
  14. Dangles, O., & Fenger, J. -A. (2018). The chemical reactivity of anthocyanins and its consequences in food science and nutrition. *Molecules*, 23(8), 1970. DOI: 10.3390/molecules23081970.
  15. Março, P. H., Poppi, R. J., Scarminio, I. S., & Tauler, R. (2011). Investigation of the pH effect and UV radiation on kinetic degradation of anthocyanin mixtures extracted from *Hibiscus acetosella*. *Food Chem.*, 125(3), 1020–1027. DOI: 10.1016/j.foodchem.2010.10.005.
  16. Indah, N. H., Listyarini, A., & Imawan, C. (2020). Natural red dyes from *Hibiscus sabdariffa* L. calyxes extract for gamma-rays detector. *J. Phys.-Conf. Ser.*, 1428(1), 012061. DOI: 10.1088/1742-6596/1428/1/012061.